

PACS numbers: 42.55.Px; 42.60.Da; 42.25.Fx
DOI: 10.1070/QE2006v036n04ABEH013141

Diffraction model of a semiconductor amplifier

D.V. Vysotsky, N.N. Elkin, A.P. Napartovich, A.G. Sukharev, V.N. Troshchieva

***Abstract*. A three-dimensional diffraction model of a semiconductor heterostructure amplifier is developed. The model describes the field propagation and optical mode establishment taking into account the amplification kinetics within the framework of the diffusion equation for current carriers in a quantum well. The results of application of this model are presented for an amplifier with an asymmetric broad waveguide and an antiwaveguide structure in the lateral direction that does not confine the field. It is shown that the length of establishment of the fundamental mode for such a structure is comparable with the length over which a weak signal is enhanced by two orders of magnitude. The balance between the gain and loss for the steady-state mode as a function of the waveguide insert width is analysed. The effect of this width on the properties of the fundamental optical mode, including the far- field intensity distribution, is studied.**

Keywords: *semiconductor laser, amplifier, mode selection, diffraction, waveguide, leaky modes.*

1. Introduction

The demand for single-mode 0.98-μm diode lasers with an output power of the order of 1 W used for pumping fibre amplifiers and for fibreless communication, has been growing in recent years. The output power of such lasers can be increased by several methods. One such methods involves an increase in the waveguide width in a direction normal to the active layer plane (transverse direction) and the use of an asymmetric arrangement of the quantum well for decreasing the overlap of the field and the amplification region [1 – 3]. This makes it possible to increase the length of the laser and hence its output power.

An increase in the width of the radiating aperture in the direction along the active layer (lateral direction) proves to be problematic due to the development of lasing at other modes. Conventional lasers employing an inbuilt waveguide (with a width up to 2 – 2.5 μm) confining the field in the lateral direction may operate in the single-mode regime at the output power up to ~0.5 W, and then lasing occurs at several modes. One of the methods of increasing the lateral dimension of the waveguide is the use of structures that do not confine the field in the lateral direction [4]. A slight increase in field losses due to its escape sideways leads to a significant increase in the pump current at which lasing becomes multimode. This allows an increase in the lateral aperture and the single-mode power. Diodes working in the amplification regime are also widely used to increase the single-mode beam power [5].

This paper is devoted to the development of a numerical three-dimensional optical model of an amplifier allowing a detailed analysis of the laser beam power balance in the presence of saturating gain and losses caused by the leakage of radiation from the active region. In addition, the numerical calculation of the radiation beam propagation in an active heterostructure is an essential component of the complete diode laser model developed simultaneously by us. The efficiency of our model is illustrated by the analysis of signal amplification in a heterostructure shown schematically in Fig. 1.

2. Numerical model

Semiconductor structures used in single-mode diode lasers consists of layers whose width considerably exceeds their thickness. The typical lengths of a structure along the optical axis are 1 – 2 mm for a width of 20 – 40 μm and a height of 2 – 4 μm. The amplification occurs in quantum wells of thickness 5 – 8 nm. This means that the spectrum of spatial scales in the problem covers five orders of magnitude. This circumstance necessitates the use of a fine network with different steps along different axes in the method of finite differences.

The propagation of radiation in the scalar approximation is described by the Helmholtz equation for the amplitude U of the monochromatic field:

$$\Delta U + (k^2 n^2 - \mathrm{i}kg)U = 0, \tag{1}$$

where $k = 2\pi/\lambda$ is the total wave number of the field in vacuum; n is the refractive index; and g is the gain which can be negative if the injection current density is lower than the density of the transparency current (injection current corresponding to the equality of amplification and absorption).

The model equations were solved by using the three-dimensional method of diffraction calculation of propagat-

D.V. Vysotsky, N.N. Elkin, A.P. Napartovich, A.G. Sukharev, V.N. Troshchieva State Research Center of the Russian Federation, Troitsk Institute for Innovation and Fusion Research, 142190 Troitsk, Moscow region, Russia; e-mail: apn@triniti.ru

Received 29 November 2005
Kvantovaya Elektronika **36** (4) 309 – 314 (2006)
Translated by Ram Wadhwa

ing beams [6, 7]. An orthogonal 256×256 grid in the laser beam cross section with a mesh size of 0.1 μm along the optical axis was employed. Thus, about $10^4 - 2 \times 10^4$ steps are required along the axis for a crystal of typical length 1 – 2 mm.

Field propagation over the structure was calculated by using the method of splitting into diffraction and refraction processes taking into account nonlinear effects [7, 8]. In order to ensure complete absorption of radiation incident at the boundaries of the computational domain, the condition of ideal matching of layers [9] in the version [10] worked out for waveguide structures was used for the lateral and transverse boundaries. It was shown in [11] that such a boundary condition is the most suitable one existing at present for simulating the physical condition for nonreflecting boundaries.

Note that the relation between the gain and the carrier concentration in a quantum well is quite complicated in the general case, and must be derived from a solution of the microscopic equations for electron and hole fluxes [12]. Because the main aim of this paper is to develop an effective optical package for the programme system, we used one of the simplest approximations for relating the gain g with the carrier concentration N in a quantum well:

$$g = g_{0N}\{[1 - \exp(-4Y^2)]\ln Y - \exp(-4Y^2)\}, \quad Y = \frac{N}{N_{\rm tr}},$$

where

$$N_{\rm tr} = \frac{-\tau_{\rm r}^{-1} + [\tau_{\rm r}^{-2} + 4BJ_{\rm tr}/(qd_{\rm w})]^{1/2}}{2B}$$

is the carrier concentration corresponding to the zero amplification/absorption; $J_{\rm tr}$ is the corresponding pump (transparency) current density; $\tau_{\rm r}$ is the linear recombination time; B is a coefficient characterising carrier losses quadratic in concentration; q is the electron charge; and $d_{\rm w}$ is the width of the quantum well. The charge carrier distribution in the quantum well along the lateral direction is determined by solving the one-dimensional diffusion equation [13]

$$\frac{\partial^2 Y}{\partial y^2} - \frac{Y}{D\tau_{\rm r}} - \frac{B}{D}N_{\rm tr}Y^2 - \frac{g}{g_{0N}D\tau_{\rm r}}|U|^2 = -\frac{J}{qDd_{\rm w}N_{\rm tr}}, \quad (2)$$

where $|U|^2 = I/I_{\rm s}$; $I_{\rm s} = hcN_{\rm tr}/(\lambda g_{0N}\tau_{\rm r})$ is the saturation intensity; h is Planck's constant; D is the diffusion coefficient for the carriers; and J is the pump current density. Losses proportional to the cube of carrier concentration (Auger recombination) were neglected in this calculation. The refractive index in the quantum well is defined as $n = n_0 - Rg/(2k)$, where n_0 is the refractive index corresponding to the transparency current, and R is the line enhancement factor. The above parameters depend on the material and specific form of the heterostructure. The values of the parameters used in this work are presented in Table 1.

Table 1. Model parameters used in calculations.

$J_{\rm tr}$/ A cm^{-2}	g_{0N}/ cm^{-1}	B/ cm^3 s^{-1}	R	$\tau_{\rm r}$/ ns	D/ cm^2 s^{-1}	$d_{\rm w}$/ nm	λ/ μm
50	2200	10^{-10}	2	1	100	8.5	0.98

3. Numerical analysis of radiation propagation in an amplifier

As an example of the application of the above-mentioned programme system, we consider the results of analysis of the operation of an amplifier with a lateral structure in the form of a system of coupled antiwaveguides [4] (fibres in which the refractive index of the core is smaller than the refractive index of the cladding). Figure 1 shows the scheme of the active zone of the device. The choice of the geometry is dictated by the fact that for a mode localised inside the central element of width d, side elements of width $d/2$ play the role of a quarter-wave plate reflecting the radiation incident on it. The refractive index and the width s of the waveguide inserts are chosen in such a way that the reflection coefficient is large for the fundamental mode field. For higher-order modes, the interference of fields outside the central element leads to an enhancement of the outer flux. Therefore, such antiwaveguide structures for all modes have higher radiation losses in the lateral directions as compared to the fundamental mode. If the input light beam is decomposed in optical modes of the given structure, it can be expected that the fundamental mode will be selected due to preferential gain and lower losses due to leakage of radiation to the boundaries of the domain.

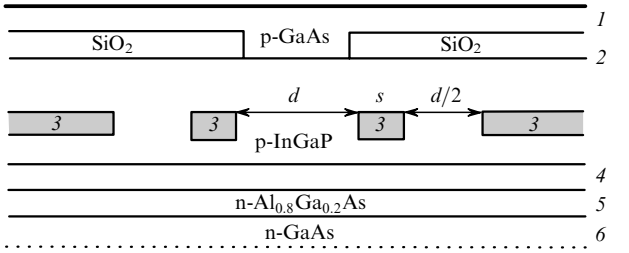

Figure 1. Scheme of the calculated region of a semiconductor amplifier (the values of thickness and refractive index are presented in Table 2): (*1*) p-contact; (*2*) p-cladding layer; (*3*) system of waveguide inserts (n-GaAs); (*4*) waveguide (heterostructure of separate confinement with a quantum well); (*5*) n-cladding layer; (*6*) substrate.

It was shown in [14] that for selecting a single mode, it is important to confine the injection current domain to the central element region. For this purpose, the material of waveguide inserts is doped in such a way as to produce electron conduction. Since the continuity equation for electric current is not solved in the model, we set the injection current density in Eqns (2) equal to a constant within the central element and zero elsewhere in the quantum well. The injection current density was normalised to the transparency current density $J_{\rm tr} = 50$ A cm^{-2}.

To study the process of fundamental mode separation, we carried out numerical calculations of the propagation of a beam having a plane wavefront at the input and a Gaussian intensity distribution with different beam sizes in transverse and lateral directions matched, respectively, with the waveguide width and the size of the central element. The heterostructure parameters are selected close to those for the structure investigated in [15]. Table 2 presents the parameters of the materials forming the heterostructure. The coefficient ε of distributed losses of radiation caused by absorption in the materials is 2 cm^{-1}, while the width d of the central element is equal to 8 μm.

Table 2. Parameters of the calculated structure with a system of coupled waveguides (see also Fig. 1).

Layer	Material	Thickness/μm	n
p-contact	p-GaAs	0.77	3.51
p-cladding layer	InGaP	0.75	3.234
Waveguide	InGaAsP	0.707	3.35
n-cladding layer	$Al_{0.8}Ga_{0.2}As$	0.75	3.085
Substrate	n-GaAs	0.4	3.51
Quantum well (inside the waveguide at a distance of 0.22 μm from its lower boundary)	InGaAs	0.007	3.7
Waveguide inserts (inside the p-cladding at a distance of 0.16 μm from its lower boundary)	n-GaAs	0.18	3.51

It should be interesting to find the gain length over which the fundamental mode is separated. Because the transverse and lateral scales of the structure differ significantly, it could be expected that transverse field distribution in the waveguide precedes lateral distribution. However, in addition to a single waveguide in the structure considered in Fig. 1, there are regions with two waveguides coupled in the transverse direction. As a result, the process of mode structure stabilisation during propagation involves a number of quite strong and interconnected variations of the field structure in transverse and lateral directions. Such variations cause irregular variations in losses associated with the escape of radiation to the boundaries as shown in Fig. 2, where the horizontal lines set the limit corresponding to the steady-state optical mode. In the first approximation, this limit is not related to the power of propagating radiation and is determined only by the process of selection of the fundamental optical mode. Apart from the losses, the overlapping of the gain region and the wave field also changes, resulting in variations in the mode gain factor that are not connected with its saturation.

Figure 3 shows the theoretical variations of the mode gain (the gain integrated over the cross section with the field intensity as the weight function) over the gain length for a structure with a waveguide insert width $s = 1.9$ μm. Large values of the distributed loss factor ($\varepsilon = 13$ cm^{-1}) for curves (*1*) and (*2*) are due to the fact that radiation losses at the input mirror are described in the calculations by the distributed loss factor equal to the threshold gain in the cavity described in [15]. An increase in the pump current [curve (*1*) in Fig. 3] leads to a more rapid gain saturation, as can be seen from a comparison of curves (*1*) and (*2*). A decrease in the losses to a value characteristic of absorption in the material (2 cm^{-1}) leads to a value of the saturated gain for curve (*3*) that is much smaller than for curve (*2*), both saturations setting in simultaneously (for a gain length $z \geqslant 0.5$ mm). The peak intensity of the input field in calculations whose results are presented in Figs 2 and 3, was $0.01I_s$. A comparison of Figs 2 and 3 shows that the length over which a single mode is selected and the length over which the gain is saturated are of the same order of magnitude for the structure under study.

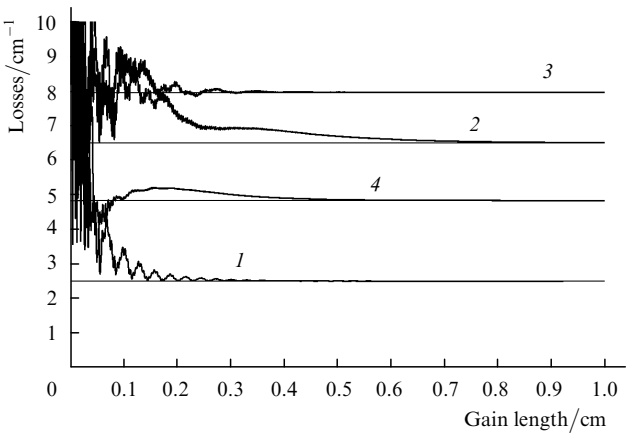

Figure 2. Losses associated with the escape of radiation to the boundaries during propagation over the amplifier for a waveguide insert width $s = 1.3$ [curve (*1*)], 1.7 [curve (*2*)], 1.9 [curve (*3*)], 2.7 μm [curve (*4*)].

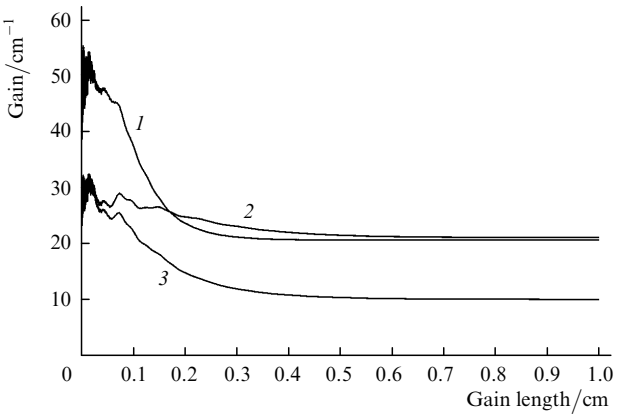

Figure 3. The gain, integrated over the cross section, as a function of the gain length for $J = 30J_{tr}$, $\varepsilon = 13$ cm^{-1} [curve (*1*)]; $J = 10J_{tr}$, $\varepsilon = 13$ cm^{-1} [curve (*2*)]; $J = 10J_{tr}$, $\varepsilon = 20$ cm^{-1} [curve (*3*)]; and $s = 1.9$ μm.

The process of separation of a single mode is illustrated in Fig. 4 which shows the logarithmic intensity levels of the field in various cross sections of a beam during its propagation for the structure with $s = 1.9$ μm. A Gaussian beam of size 0.35 μm in the transverse direction (along the x axis) and 8 μm in the lateral direction (along the y axis) supplied at the input is considerably modified over distances of tens of micrometers (for the sake of convenience of visualisation, quite different scales are chosen for the x and y axes). Typical field distribution in the form of a single central spot and two side spots in the lateral direction and spots of radiation flowing into additional waveguides is formed after the passage of the beam through the first ten micrometers. However, the shape of both central spot and side spots changes subsequently, and the field is redistributed between the main and additional waveguides. The last frame in Fig. 4 shows the steady-state distribution of the mode intensity.

It is interesting to note that in spite of the structural rearrangement of the field during its propagation, the beam amplification is described with reasonable accuracy by the simplest one-dimensional model of radiation transport, the intensity dependence of the gain being approximated by the Rigrod formula [16].

The transport equation for the total emission power P has the form

$$\frac{dP}{dz} = (G - \alpha)P, \tag{3}$$

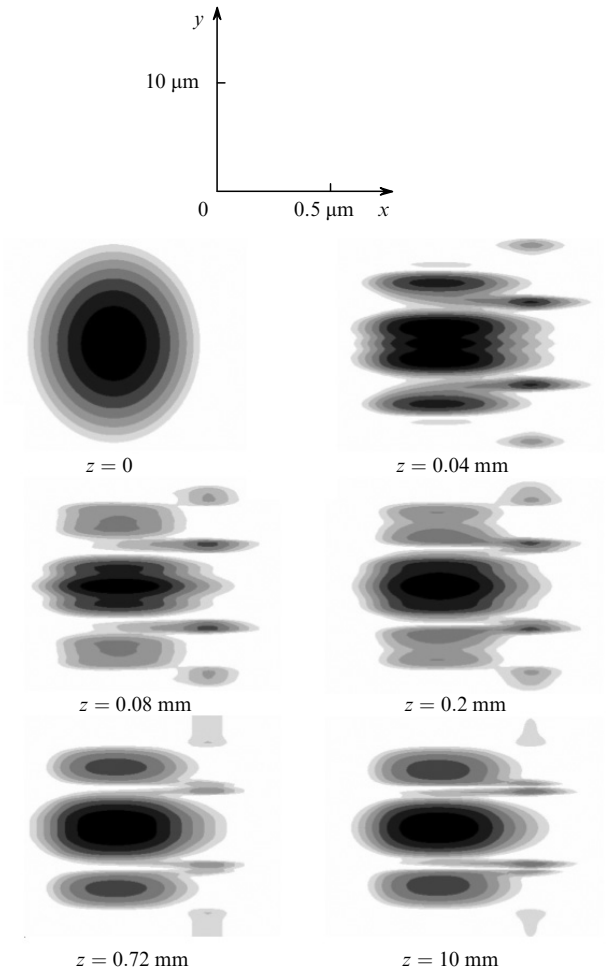

Figure 4. Emission intensity distribution over the beam aperture for various gain lengths for $s = 1.9$ μm.

where G is the gain for the total beam and α is the integral distributed loss factor. By using the Rigrod formula $G = G_0/(1 + P/P_s)$, Eqn (3) can be solved quite easily and its solution gives the following relation between the total beam power and the gain length z:

$$(G_0 - \alpha)z = \ln\frac{P}{P_0} - \frac{G_0}{\alpha}\ln\frac{[(G_0/\alpha) - 1 - P/P_s]}{[(G_0/\alpha) - 1 - P_0/P_s]}, \qquad (4)$$

where G_0 is the small-signal gain; P_0 is the input signal power; and P_s is the saturation power. The total numerical calculation of the gain of the input signal with a peak intensity $0.01I_s$ for an absorption coefficient in the material equal to 2 cm^{-1} leads to a dependence of the total amplified signal on the distance shown by the solid curve in Fig. 5. The total amplification of the beam over the entire length is $P/P_0 \approx 1500$. Considerable saturation of the extracted power level occurs over a length of the order of 5 mm.

Recall that the quantities G_0, α, P_0, and P_s in expression (4) are integrated parameters of beam propagation in the medium. The distributed loss factor α includes absorption losses in the material as well as losses due to the leakage of radiation. The difference $G_0 - \alpha$ was determined from the results of numerical calculations for the small-signal gain mode, while the ratio G_0/α was obtained from calculations for the complete saturation mode. The following values of parameters were obtained: $\alpha = 10$ cm^{-1}, $G_0 = 31.4$ cm^{-1}, $P_0/P_s = 1.35 \times 10^{-3}$. Using dependence (4) with the parameters determined in this way, we plotted the dashed curve in Fig. 5. A slight difference between the two curves in this figure indicates that the establishment of the mode structure of the beam accompanied by variations in the loss (Fig. 2) and gain (Fig. 3) does not noticeably affect the energetics of the gain.

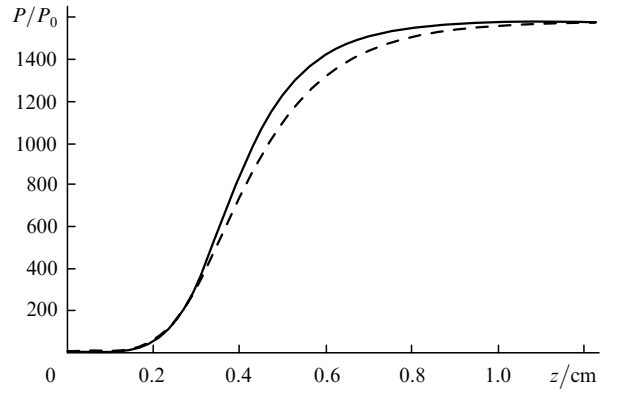

Figure 5. Radiation beam power normalised to the input power as a function of the beam length. The solid curve corresponds to total numerical calculation for a peak intensity of $0.01I_s$ and an absorption in the material equal to 2 cm^{-1}. The dashed curve was plotted using formula (4) for $\alpha = 10$ cm^{-1}, $G_0 = 31.4$ cm^{-1} and $P_0/P_s = 1.35 \times 10^{-3}$.

Numerical analysis of an analogous diode structure [17] working in the generator regime shows that the width s of the waveguide inserts is an important structural parameter that determines to a considerable extent the stability of the single-mode laser operation. In order to find how the variation of parameter s affects the balance between the radiation gain and loss, we made a number of calculations by varying the value of s for the above-mentioned amplifier.

In this series of calculations, we fixed the values of the injection current density (at 500 A $cm^{-2} = 10J_{tr}$) and the coefficient of distributed losses imitating the emergence of radiation through the mirrors (13 cm^{-1}). Calculations were made until approaching the steady-state regime in which the saturated gain becomes equal to the overall losses including the distributed losses (13 cm^{-1}) and the losses due to leakage of radiation to the substrate and in the lateral direction. The histogram presented in Fig. 6 shows the theoretical dependence of the overall radiation losses (total height of the

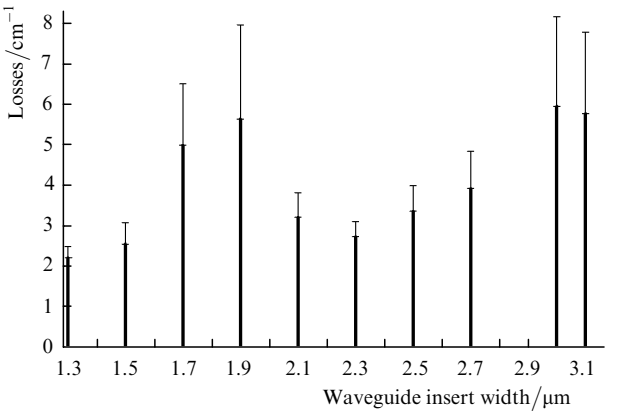

Figure 6. Losses due to escape of radiation in the transverse (thick part of the columns) and lateral (thin part of the columns) directions for various values of s.

columns) as well as the fraction of losses due to the escape of radiation in the transverse (thick part of the columns) and lateral (thin part of the columns) directions. At all points, losses due to the escape of radiation in the transverse direction dominate. It is interesting to note that the 'lateral' and 'transverse' radiation losses behave in an analogous manner upon a variation of s, although the relative variation of 'lateral' losses is noticeably higher.

One can see from Fig. 6 that radiation losses change quite significantly upon a variation of the width of waveguide inserts. This means that the threshold pump current depends strongly on s. The strong dependence of losses and threshold current on parameter s is due to structural rearrangement of the generated mode shown in Fig. 7. The rearrangement mainly involves a variation in the field structure inside the waveguide inserts and of field intensity in the side elements. The relative increase in the field intensity in the side elements and waveguide inserts leads to lateral and transverse radiation losses. Moreover, a variation in the parameter s changes the phase difference between fields in central and side elements. One can see from Fig. 8 that this considerably varies the field distribution in the far-field zone in the lateral direction. For $s = 1.3$, 1.7 and 3.1 μm, the phase of the field in the transverse direction is opposite to that of the field in the central element, and, hence, an intensity dip emerges on the axis, its depth depending on the ratio of intensities at the centre and side elements.

For $s = 1.9$, 2.3 and 2.7 μm, the field has its highest value on the axis, since the fields in the central and side elements are in phase. The change in the width of the central peak and the relative height of lateral orders in the intensity distribution in the far-field zone is due to a variation of the relative height of the field intensity peaks in side elements (see Fig. 7). Composition of beams of comparable intensities for $s = 1.9$ μm narrows the peak in the far-field zone since the effective radiating aperture is quite large in this case. Accordingly, the field intensity in side elements is low for $s = 2.3$ μm. The width of the central peak in the far-field zone becomes larger due to a decrease in the effective radiating aperture. The position of the first lateral orders in the far-field zone is determined by the distance between the axis and the middle of the side element, and their height depends on the relative height of the intensity peaks in the side elements. These correlations can be seen clearly by comparing Figs 7 and 8.

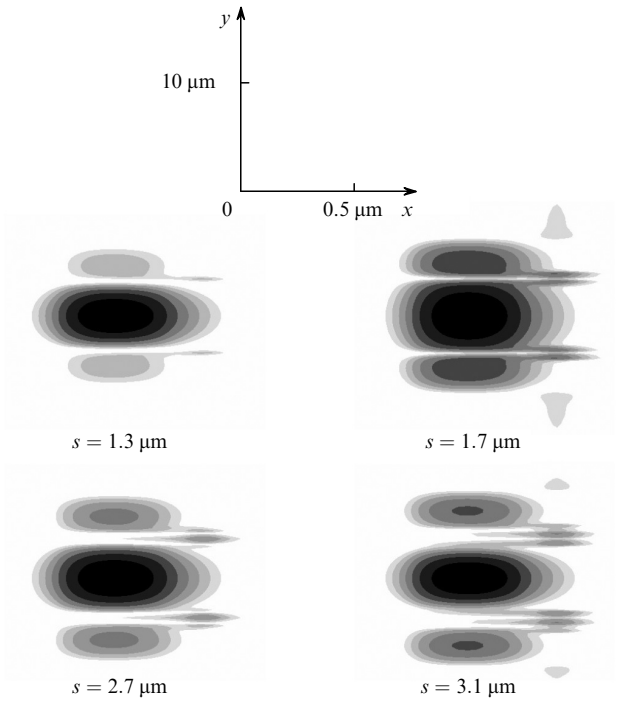

Figure 7. Distribution of the radiation field in the near-field zone after passing through a 1-mm-long amplifier for various values of s.

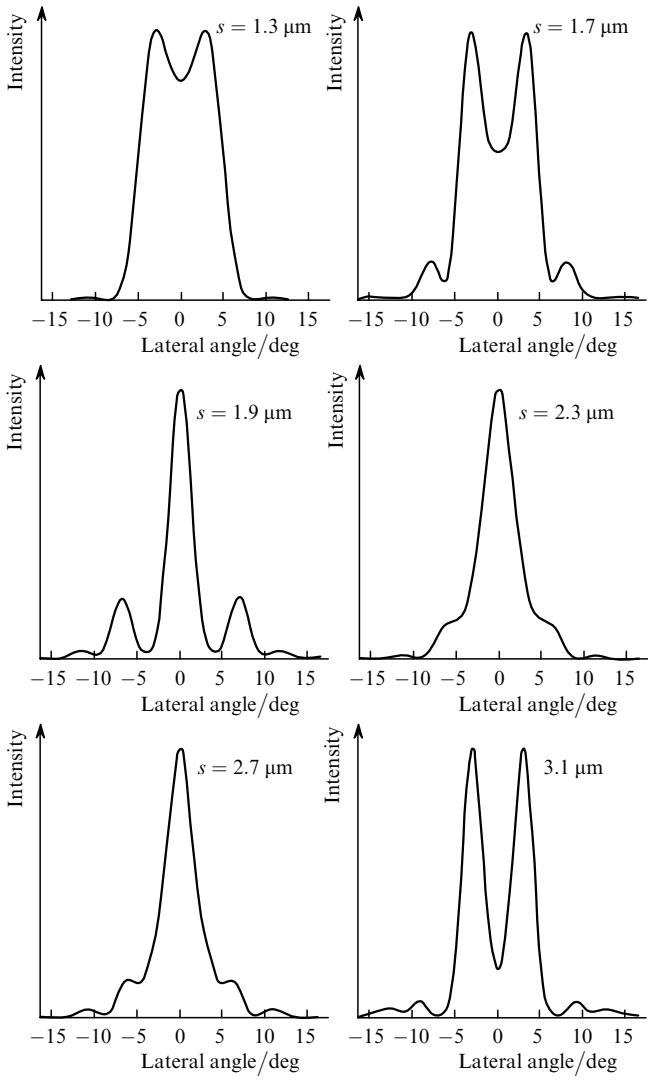

Figure 8. Field intensity profile in the far-field zone after passing through a 1-mm-long amplifier for various values of s.

For the chosen structural parameters, the loss associated with the escape of radiation to the boundaries varies from 2.5 to 8.2 cm^{-1} depending on the width of the waveguide inserts (see Fig. 6). For such values of the loss, the reasonable gain length (in the absence of absorption in the materials) is confined to values $\sim 1 - 4$ mm. Upon a further increase in the gain length, all the radiation will escape to the walls. The radiative losses may be reduced by increasing the thickness of the cladding layers. Numerical calculations for a structure with $s = 2.3$ μm (corresponding to the minimum loss in Fig. 6) show that an increase in the thickness of the p- and n-cladding layers from 0.75 to 1 μm

and from 0.75 to 0.9 μm, respectively, leads to a decrease in the radiative loss factor from 3.08 to 0.85 cm^{-1}. Calculations were made for a pump current density of 200 A cm^{-2} = $4J_{tr}$. In this case, the output emission power over a length of 1 cm increased by a factor of 1.7. The total losses are reduced mainly due to a decrease in 'transverse' losses. While the fraction of losses due to lateral emission was 12 % in the initial structure, its value increases to 67 % due to an increase in the cladding layer thickness. Note that the field structure of the optical mode remains virtually unchanged in this case. The problem of an increase in the admissible losses is connected with the stability of single-mode regime upon an increase in the pump level and must be solved separately [17].

Only order-of-magnitude estimates are available for the parameters appearing in the diffusion equation (2). In particular, the diffusion coefficient, which considerably affects the gain profile in a quantum well, may turn out to be smaller than the value 100 cm^2 s^{-1} chosen by us. Calculations made for $D = 50$ cm^2 s^{-1} show that the output power increases by 8 % in this case, while the losses remain virtually at the same level.

4. Conclusions

We have described a three-dimensional diffraction programme for simulating semiconductor amplifiers. This programme is based on the solution of the scalar wave equation in paraxial optics approximation and the diffusion equation for carriers in a quantum well. The results of its application for an amplifier with a heterostructure forming a system of coupled antiwaveguides in the lateral direction are presented. It is shown that the length over which the fundamental mode is established in such a structure is comparable with the length over which a weak signal is amplified by two orders of magnitude. It is found that, in spite of a considerable variation of the field structure at the stage of predominant mode extraction, the energy parameters of the amplifier are defined by a simple approximation. The balance between loss and gain for the established mode as a function of the waveguide insert width is analysed. Structural variations of the dominating optical mode in the near- and far-field zones upon a variation of the width s of the inserts are numerically examined. Values of s ensuring a small angular divergence in the lateral direction are derived.

Acknowledgements. This work was supported by the Russian Foundation for Basic Research (Grant No. 05-02-16769) and 'Leading Research Schools' (Grant No. RI-112/001/593). The authors thank D. Botez and L. Mawst of Wisconsin-Madison University for initiating this research.

References

1. Gokhale M.R., Dries J.C., Studenkov P.V., Forrest S.R., Garbuzov D.Z. *IEEE J. Quantum Electron.*, **33**, 2266 (1997).
2. Al-Muhanna A., Mawst L.J., Botez D., Garbuzov D.Z., Martinelli R.U., Connoly J.C. *Appl. Phys. Lett.*, **73**, 1182 (1998).
3. Slipchenko S.O., Pikhtin N.A., Fetisova N.V., Khomylev M.A., Marmalyuk A.A., Nikitin B.B., Padalitsa A.A., Bulaev P.V., Zalevskii I.D., Tarasov I.S. *Pis'ma Zh. Tekh. Fiz.*, **29**, 26 (2003).
4. Mawst L.J., Botez D., Zmudzinski C., Tu C. *Appl. Phys. Lett.*, **61**, 503 (1992).
5. Welch D.F., Mehuys D.G., in *Diode Laser Arrays*. Ed. by D. Botez and D.R. Scifres (Cambridge University Press, 1994) pp 72–122.
6. Scarmozzino R., Gopinath A., Pregla R., Helfert S. *IEEE J. Sel. Top. Quantum Electron.*, **6** (1), 150 (2000).
7. Elkin N.N., Napartovich A.P., Sukharev A.G., et al. *Opt. Commun.*, **177**, 207 (2000).
8. Elkin N.N., Napartovich A.P., Sukharev A.G., Vysotsky D.V. *Lect. Notes in Comp. Sci.*, **3401**, 272 (2005).
9. Berenger J.P. *J. Comp. Phys.*, **114**, 185 (1994).
10. Huang W.P., Xu C.G., Lui W., Yokoyama K. *IEEE Photon. Techn. Lett.*, **8**, 652 (1996).
11. Fogli F., Bellanca G., Bassi P. *J. Opt. Quantum Electron.*, **30**, 443 (1998).
12. Coldren L.A., Corzine S.W. *Diode Lasers and Photonic Integrated Circuits* (New York: Wiley, 1995).
13. Hadley G.R., Hohimer J.P., Owyoung A. *IEEE J. Quantum Electron.*, **23**, 765 (1988).
14. Mawst L.J., Botez D., Nabiev R.F., Zmudzinski C. *Appl. Phys. Lett.*, **66** (1), 7 (1995).
15. Chang J.C., Lee J.J., Al-Muhanna A., Mawst L.J., Botez D. *Appl. Phys. Lett.*, **81**, 1 (2002).
16. Rigrod W.W. *J. Appl. Phys.*, **36**, 2487 (1965).
17. Napartovich A.P., Elkin N.N., Sukharev A.G., et al. *Proc. SPIE Int. Soc. Opt. Eng.*, **5722**, 267 (2005).